

Scaled relative graphs for system analysis

Thomas Chaffey¹

Fulvio Forni¹

Rodolphe Sepulchre¹

Abstract—Scaled relative graphs were recently introduced to analyze the convergence of optimization algorithms using two dimensional Euclidean geometry. In this paper, we connect scaled relative graphs to the classical theory of input/output systems. It is shown that the Nyquist diagram of an LTI system on L_2 is the convex hull of its scaled relative graph under a particular change of coordinates. The SRG may be used to visualize approximations of static nonlinearities such as the describing function and quadratic constraints, allowing system properties to be verified or disproved. Interconnections of systems correspond to graphical manipulations of their SRGs. This is used to provide a simple, graphical proof of the classical incremental passivity theorem.

I. INTRODUCTION

The Scaled Relative Graph (SRG) of Ryu, Hannah, and Yin [1] allows the action of a nonlinear operator to be visualized on the complex plane. Incremental properties of an operator, measured between pairs of inputs and outputs, such as maximal monotonicity and Lipschitz continuity, may be verified by checking geometric conditions on the SRG of the operator. Algebraic manipulations to the operator correspond to geometric manipulations to the SRG. This tool allows simple, intuitive and rigorous proofs of the convergence of many algorithms in convex optimization. Furthermore, the graphical method is particularly suitable for proving tightness of convergence bounds, with several novel tightness results being proved [1], [2].

In this paper, we connect the scaled relative graph to the classical theory of input/output systems. The SRG of a linear, time invariant operator is the convex hull of its Nyquist diagram under a particular change of coordinates. The Nyquist diagram is a cornerstone of linear system theory, and has given rise to many fundamental developments in the field, among them the Nyquist stability criterion [3], the definition of stability margins and system robustness, the gap metric [4] and graphical interpretation of H_∞ control [5]. The Nyquist diagram also has a fundamental place in the theory of nonlinear systems of the Lur'e form (that is, systems composed of an LTI forward path in feedback with a static nonlinearity). The circle and Popov criteria allow the stability of a Lur'e system to be proved by verifying a geometric condition on the Nyquist diagram of the LTI component [6]. The geometric condition is determined by the properties of the static nonlinearity. Notably, only the

The research leading to these results has received funding from the European Research Council under the Advanced ERC Grant Agreement Switchlet n. 670645.

¹The authors are with the University of Cambridge, Department of Engineering, Trumpington Street, Cambridge CB2 1PZ, tlc37@cam.ac.uk, f.forni@eng.cam.ac.uk, r.sepulchre@eng.cam.ac.uk.

Nyquist diagram of the LTI component is well-defined, owing to a lack of a suitable definition of phase for nonlinear systems. This clearly hampers the use of the Nyquist diagram in nonlinear system theory. A notable, classical extension of the Nyquist diagram to nonlinear systems is the describing function [7]–[9]. This approximate method produces a family of Nyquist curves for a nonlinearity, parameterized by the amplitude of the input. Other efforts to generalize frequency response to nonlinear systems include the work of Pavlov, van de Wouw, and Nijmeijer [10] on Bode diagrams for convergent systems, and the recently introduced notion of nonlinear phase by Chen, Zhao, Chen, *et al.* [11].

Whilst the SRG generalizes the Nyquist diagram of an LTI operator, it may be plotted for any nonlinear operator, allowing the use of graphical techniques for the analysis of arbitrary interconnected systems. We anticipate that, in the same way as the SRG allows simple, graphical proofs of many results in optimization, the SRG will allow simple, graphical proofs of the incremental versions of many classical results in nonlinear systems and control. Furthermore, it will allow the popular graphical control design techniques for LTI systems to be extended to nonlinear systems.

In this preliminary work, we make the first steps towards these aims. We begin in Section II by defining the SRG over a Hilbert space, and showing how several important system properties can be determined from the SRG. We then characterize the SRG of an LTI operator on L_2 in Section III. In Section IV, we examine the SRGs of static nonlinearities, and show that standard approximations of static nonlinearities, such as the describing function and quadratic constraints, have readily computed SRGs which under- and over-approximate the SRG of the true system. Finally, in Section V we demonstrate the usefulness of the SRG in the analysis of interconnected systems with a simple, graphical proof of the incremental passivity theorem.

II. SCALED RELATIVE GRAPHS

We define SRGs in the same way as Ryu, Hannah, and Yin [1], with the minor modification of allowing complex valued inner products. Let \mathcal{H} be a Hilbert space, equipped with an inner product, $\langle \cdot | \cdot \rangle : \mathcal{H} \times \mathcal{H} \rightarrow \mathbb{C}$, and the induced norm $\|x\| := \sqrt{\langle x | x \rangle}$.

The angle between $x, y \in \mathcal{H}$ is defined as

$$\angle(x, y) := \arccos \frac{\operatorname{Re} \langle x | y \rangle}{\|x\| \|y\|}.$$

Let $R : \mathcal{H} \rightarrow \mathcal{H}$ be an operator, or *system*. Given $u_1, u_2 \in$

$\mathcal{U} \subseteq \mathcal{H}$, define the complex number $z_R(u_1, u_2)$ by

$$z_R(u_1, u_2) := \frac{\|Ru_1 - Ru_2\|}{\|u_1 - u_2\|} e^{j\angle(u_1 - u_2, Ru_1 - Ru_2)}.$$

The *Scaled Relative Graph* (SRG) of R over $\mathcal{U} \subseteq \mathcal{H}$ is then given by

$$\text{SRG}_{\mathcal{U}}(R) := \{z_R(u_1, u_2) | u_1, u_2 \in \text{dom}R, u_1 \neq u_2\}.$$

If $\mathcal{U} = \mathcal{H}$, we write $\text{SRG}(R) := \text{SRG}_{\mathcal{H}}(R)$.

If R is linear and $\text{dom}R$ is a linear subspace of \mathcal{H} , $Ru_1 - Ru_2 = R(u_1 - u_2) = R(v)$ for some $v \in \text{dom}R$, and we can define

$$z_R(v) := \frac{\|Rv\|}{\|v\|} e^{j\angle(v, Rv)}$$

and

$$\text{SRG}_{\text{dom}R}(R) := \{z_R(v) | v \in \text{dom}R, v \neq 0\}.$$

Each point on the SRG of an operator shows the gain and phase shift of a particular pair of inputs. The SRG thus allows the gain and phase shift of nonlinear operators to be visualized graphically, similar to the Nyquist diagram of an LTI transfer function.

If \mathcal{A} is a class of operators, we define the SRG of \mathcal{A} by

$$\text{SRG}(\mathcal{A}) := \bigcup_{R \in \mathcal{A}} \text{SRG}(R).$$

A class \mathcal{A} , or its SRG, is called *SRG-full* if

$$R \in \mathcal{A} \iff \text{SRG}(R) \subseteq \text{SRG}(\mathcal{A}).$$

By construction, the implication $R \in \mathcal{A} \implies \text{SRG}(R) \subseteq \text{SRG}(\mathcal{A})$ is true. The value of SRG-fullness is in the reverse implication: $\text{SRG}(R) \subseteq \text{SRG}(\mathcal{A}) \implies R \in \mathcal{A}$. This allows class membership to be tested graphically. If \mathcal{A} is the class of systems with a particular system property, SRG-fullness of \mathcal{A} allows this property to be verified for a particular operator R by plotting its SRG. If $\text{SRG}(R) \subseteq \text{SRG}(\mathcal{A})$, R has the property.

We demonstrate this approach using two classical system properties: L_2 gain and incremental positivity (or monotonicity). Let $L_2(\mathbb{F})$ be the space of square-integrable signals with values in the field $\mathbb{F} \in \{\mathbb{R}, \mathbb{C}\}$. We write L_2 when the choice of field is immaterial. Define the usual inner product and norm by

$$\langle u | y \rangle := \int_{-\infty}^{\infty} u(t) \bar{y}(t) dt, \\ \|u\| := \sqrt{\langle u | u \rangle},$$

where $\bar{y}(t)$ denotes the complex conjugate of $y(t)$.

Let $R: L_2 \rightarrow L_2$. R is said to have an *incremental L_2 norm bound of γ* [12] if

$$\|Ru_1 - Ru_2\| \leq \gamma \|u_1 - u_2\|$$

for all $u_1, u_2 \in L_2$. R is said to be *incrementally positive*, or *monotone on L_2* , if

$$\langle u_1 - u_2 | Ru_1 - Ru_2 \rangle \geq 0$$

for all $u_1, u_2 \in L_2$. Note that incremental positivity here is meant in the operator theoretic sense of [6, sec 4 p. 173]. It is closely related to incremental passivity - indeed, if R is causal, the two are equivalent (the proof is identical to that of [6, Lem. 2, p. 200]). Furthermore, if a system is linear and time-invariant, incremental passivity is equivalent to passivity.

The following two propositions demonstrate the verification of system properties from the system's SRG, and follow directly from [1, Prop. 3.3 & Thm. 3.5]. Both incremental L_2 gain and incremental positivity define SRG-full classes.

Proposition 1. *An operator $R: L_2 \rightarrow L_2$ has an incremental L_2 gain less than γ if and only if its SRG lies within the circle centred at the origin of radius γ .*

This property is reminiscent of the property that the L_2 gain of an LTI transfer function is the maximum magnitude of its frequency response.

Proposition 2. *An operator $R: L_2 \rightarrow L_2$ is incrementally positive if and only if its SRG lies in the right half plane, $\mathbb{C}_{\text{Re} \geq 0}$.*

This property is reminiscent of the positive realness of a transfer function.

The properties of bounded incremental L_2 gain and incremental positivity are particular examples of incremental Integral Quadratic Constraints (IQCs) [13]. A striking corollary of Ryu, Hannah, and Yin [1, Thm. 3.5] is that any SRG defined by a frequency-independent incremental IQC is SRG-full.

Proposition 3. *Let $u_i(t)$ denote the input to an arbitrary operator on L_2 , and $y_i(t)$ denote the corresponding output. Let $\Delta u = u_1 - u_2$ and $\Delta y = y_1 - y_2$, and $\hat{x}(\omega)$ denote the Fourier transform of signal $x(t)$. Then the classes of operators which obey either of the constraints*

$$\int_{-\infty}^{\infty} \begin{pmatrix} \Delta \hat{u}(\omega) \\ \Delta \hat{y}(\omega) \end{pmatrix}^T \begin{pmatrix} a & b \\ c & d \end{pmatrix} \begin{pmatrix} \Delta \hat{u}(\omega) \\ \Delta \hat{y}(\omega) \end{pmatrix} d\omega \geq 0, \quad (1)$$

$$\int_{-\infty}^{\infty} \begin{pmatrix} \Delta u(t) \\ \Delta y(t) \end{pmatrix}^T \begin{pmatrix} a & b \\ c & d \end{pmatrix} \begin{pmatrix} \Delta u(t) \\ \Delta y(t) \end{pmatrix} dt \geq 0, \quad (2)$$

where $a, b, c, d \in \mathbb{R}$, are SRG-full.

Proof. Equation (1) gives

$$a \|\Delta \hat{u}\|^2 + (b+c) \langle \Delta \hat{u} | \Delta \hat{y} \rangle + d \|\Delta \hat{y}\|^2 \geq 0.$$

By Parseval's theorem, this is equivalent to

$$a \|\Delta u\|^2 + (b+c) \langle \Delta u | \Delta y \rangle + d \|\Delta y\|^2 \geq 0,$$

which is also implied by (2). The result then follows from [1, Thm. 3.5]. \square

III. SCALED RELATIVE GRAPHS OF LTI SYSTEMS

In this section, we investigate the relationship between the SRG of an LTI system and the classical tool of the Nyquist diagram. Huang, Ryu, and Yin [14] show that the SRG of a diagonal matrix A is the convex hull of the points $z_A(u_i)$,

where u_i are the eigenvectors of A , and the convex hull is taken under the Beltrami-Klein change of coordinates. Here, we develop the analogous result for LTI operators on $L_2(\mathbb{C})$. We show that the SRG of such an LTI operator is the convex hull of its Nyquist diagram, under the same nonlinear change of coordinates.

A. Hyperbolic geometry

We recall some necessary details from hyperbolic geometry. The notation we use is consistent with Huang, Ryu, and Yin [14].

Definition 1. Let $z_1, z_2 \in \mathbb{C}_{\text{Im} \geq 0} := \{z \in \mathbb{C} \mid \text{Im}(z) \geq 0\}$, the upper half complex plane. We define the following subsets of $\mathbb{C}_{\text{Im} \geq 0}$:

- 1) $\text{Circ}(z_1, z_2)$ is the circle through z_1 and z_2 with centre on the real axis. If $\text{Re}(z_1) = \text{Re}(z_2)$, this is defined as the line extending $[z_1, z_2] := \{\alpha z_1 + (1 - \alpha)z_2 \mid \alpha \in [0, 1]\}$.
- 2) $\text{Arc}_{\min}(z_1, z_2)$ is the arc of $\text{Circ}(z_1, z_2)$ in $\mathbb{C}_{\text{Im} \geq 0}$. If $\text{Re}(z_1) = \text{Re}(z_2)$, then $\text{Arc}_{\min}(z_1, z_2)$ is $[z_1, z_2]$ (which is the singleton $\{z_1\}$ if $z_1 = z_2$).
- 3) Given $z_1, \dots, z_m \in \mathbb{C}_{\text{Im} \geq 0}$, the *arc-edge polygon* is defined by: $\text{Poly}(z_1) := \{z_1\}$ and $\text{Poly}(z_1, \dots, z_m)$ is the smallest simply connected set containing S , where

$$S = \bigcup_{i,j=1\dots m} \text{Arc}_{\min}(z_i, z_j).$$

⌋

Note that, as $\text{Poly}(z_1, \dots, z_{m-1}) \subseteq \text{Poly}(z_1, \dots, z_{m-1}, z_m) \subseteq \mathbb{C}_{\text{Im} \geq 0}$, the set $\text{Poly}(Z)$, where Z is a countably infinite sequence of points in $\mathbb{C}_{\text{Im} \geq 0}$, is well defined (by the monotone convergence theorem) as the limit $\lim_{m \rightarrow \infty} \text{Poly}(Z_m)$, where Z_m is the length m truncation of Z .

The notions of Definition 1 form the basis of the Poincaré half plane model of hyperbolic geometry. Under the Beltrami-Klein mapping, $\mathbb{C}_{\text{Im} \geq 0}$ is mapped onto the unit disc, and $\text{Arc}_{\min}(z_1, z_2)$ is mapped to a straight line segment. The Beltrami-Klein mapping is given by $f \circ g$, where

$$f(z) = \frac{2z}{1 + |z|^2},$$

$$g(z) = \frac{z - i}{z + i}.$$

We make the following definitions of convexity and the convex hull in the Poincaré half plane model.

Definition 2. A set $S \subseteq \mathbb{C}_{\text{Im} \geq 0}$ is called *hyperbolic-convex* or *h-convex* if

$$z_1, z_2 \in S \implies \text{Arc}_{\min}(z_1, z_2) \in S.$$

Given a set of points $P \in \mathbb{C}_{\text{Im} \geq 0}$, the *h-convex hull* of P is the smallest h-convex set containing P . ⌋

Note that h-convexity is equivalent to Euclidean convexity under the Beltrami-Klein mapping. $\text{Arc}_{\min}(z_1, z_2)$ is the minimal geodesic between z_1 and z_2 under the Poincaré metric, so h-convexity may be thought of as geodesic convexity with respect to this metric.

B. LTI SRGs and the Nyquist diagram

Let $g : L_2(\mathbb{C}) \rightarrow L_2(\mathbb{C})$ be linear and time invariant, and denote its transfer function by $G(s)$. g maps a complex sinusoid $u(t) = ae^{j\omega t}$ to the complex sinusoid¹ $y(t) = |G(j\omega)|e^{j\omega t}e^{-G(j\omega)+j\omega t}$.

Definition 3. The Nyquist diagram $\text{Nyquist}(G)$ of an operator $g : L_2(\mathbb{C}) \rightarrow L_2(\mathbb{C})$ is the locus of points $\{G(j\omega) \mid \omega \in \mathbb{R}\}$. ⌋

Theorem 1. Let $g : L_2(\mathbb{C}) \rightarrow L_2(\mathbb{C})$ be linear and time invariant. $\text{SRG}(G) \cap \mathbb{C}_{\text{Im} \geq 0}$ is the h-convex hull of $\text{Nyquist}(G) \cap \mathbb{C}_{\text{Im} \geq 0}$.

The proof of Theorem 1 is closely related to the proof of Huang, Ryu, and Yin [14, Thm. 3.1], and may be found in the submitted journal version of this paper [15]. A consequence of Theorem 1 is that the SRG of an LTI operator is bounded by its Nyquist diagram.

Given Theorem 1, we recover the following two familiar properties of the Nyquist diagram as special cases of Propositions 1 and 2.

Corollary 1. The L_2 gain of a stable transfer function $G(s)$ is the largest magnitude of its Nyquist diagram, $\max_{\omega \in \mathbb{R}} |G(j\omega)|$.

Corollary 2. A causal transfer function $G(s)$ is passive if and only if its Nyquist diagram lies in the right half plane.

The Nyquist diagram of the first order lag

$$G(s) = \frac{1}{s+1}$$

is the circle in \mathbb{C} with centre 0.5 and radius 0.5 (Figure 1, top). Under the Beltrami-Klein transformation, this is a straight line (which is evident as it is a circle with centre on the real axis), and is therefore its own h-convex hull (Figure 1, bottom). It follows that $\text{SRG}(G) = \text{Nyquist}(G)$.

Two examples of transfer functions whose Nyquist diagrams are proper subsets of their SRGs are illustrated in Figures 2 and 3. These are the systems $1/(s^2 + 2s + 1)$ and $1/(s^3 + 5s^2 + 2s + 1)$ respectively. The upper plots illustrate the SRGs, while the lower plots show the corresponding regions under the Beltrami-Klein mapping.

IV. SCALED RELATIVE GRAPHS OF STATIC NONLINEARITIES

The second class of systems we consider are static nonlinearities, that is, systems governed by a relation

$$y(t) = \phi(u(t))$$

between the input at time t and the output at time t . In general, it is difficult to analytically compute the SRG of a static nonlinearity. However, valuable information about a system can be obtained from under- and over-approximations

¹While these complex exponentials do not belong to $L_2(\mathbb{C})$, they can be treated as the limit of a series of signals in $L_2(\mathbb{C})$ (for example, truncations to a finite number of periods), and their inner products can be computed accordingly.

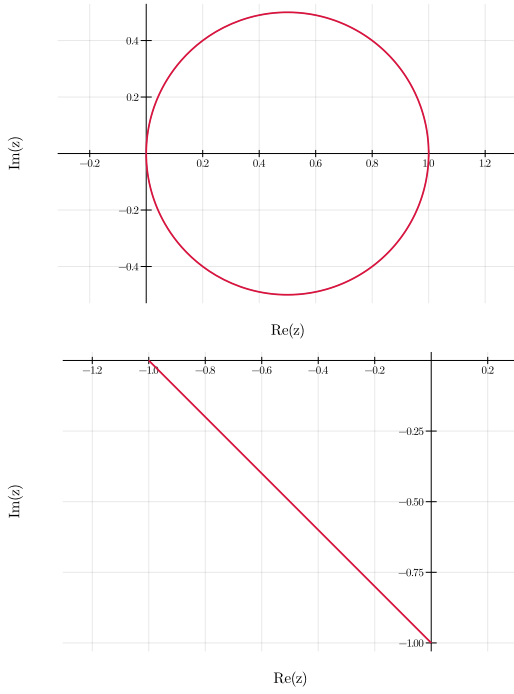


Fig. 1. The SRG of the first order lag $1/(s+1)$ is its Nyquist diagram (top). Under the Beltrami-Klein mapping, the upper half of the Nyquist diagram maps to a straight line on the unit disc (bottom).

of its SRG. In this section, we describe several methods for approximating the SRG of a static nonlinearity, demonstrated on the running example of a saturation, $y = \text{sat}(u)$:

$$\text{sat}(u) := \begin{cases} -1 & u < -1 \\ u & |u| \leq 1 \\ 1 & u > 1. \end{cases}$$

A. Sampling the scaled relative graph

The simplest method of approximating the SRG of a system is to sample the input space and directly compute the SRG over these samples, producing a subset of the full SRG.

Fourier analysis allows the computation of the SRG over individual samples to be made more computationally tractable. While computing the inner product over a continuous signal may in general be expensive, by Parseval's theorem, we have $\langle u|y \rangle = \langle \hat{u}|\hat{y} \rangle$, where \hat{x} represents the Fourier transform of x . If the input signals are chosen to have a small number of nonzero Fourier coefficients (like, for example, sinusoids), inner products involving the inputs u_1, u_2 can be computed using a small number of arithmetic operations. However, for a nonlinear system, the spectrum of the output may still be infinite. The action of the nonlinear system can be approximated by restricting to a finite number of harmonics of the output.

The classical method of describing function analysis approximates the response of a nonlinear system, excited by a sinusoidal input, by the fundamental frequency component of the output [7]. This provides a generalization of a

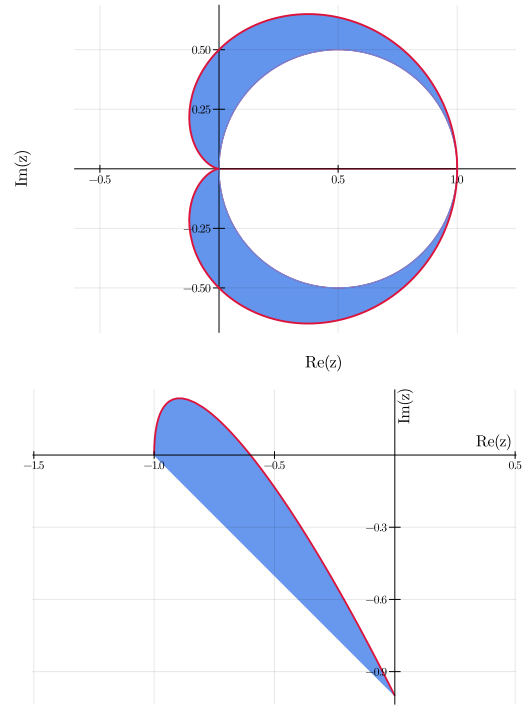


Fig. 2. SRG of the transfer function $1/(s^2 + 2s + 1)$ (top). The red curve is its Nyquist diagram. The image of the upper half of the SRG under the Beltrami-Klein mapping is shown below.

transfer function which is, in general, dependent on both the amplitude and frequency of the input sinusoid. If higher harmonics are filtered out by other components of the system, this provides a reasonable approximation of the nonlinear operator [8], [9].

Let $R: L_2(\mathbb{C}) \rightarrow L_2(\mathbb{C})$ be a nonlinear operator, $u(t) = ae^{j\omega t}$ and $y(t) = Ru(t)$. If R is a static nonlinearity, y will be periodic with the same period as u , and can be expanded in the Fourier series $y(t) = \sum_{n=0}^{\infty} \hat{y}(n) e^{jn\omega t}$. The describing function of R is defined as $\text{DF}(R)(a, \omega) = \hat{y}(1)/a$. The describing function defines an operator $\text{DF}(R)$ on the set of complex exponentials by $ae^{j\omega t} \mapsto \text{DF}(R)(a, \omega) ae^{j\omega t}$. This operator can be visualized on an SRG by restricting inputs u_1, u_2 to be of the form $u_i(t) = a_i e^{j\omega_i t + j\psi_i}$.

For several common nonlinearities of practical importance, the describing function can be computed analytically - see, for example, [9]. The describing function of the saturation is given by

$$\text{DF}(\text{sat}(u))(a) = \begin{cases} 1 & |a| < 1 \\ \frac{2}{\pi} \left(\text{asin} \frac{1}{a} + \frac{1}{a} \sqrt{1 - \frac{1}{a^2}} \right) & |a| > 1. \end{cases}$$

The SRG of this describing function is illustrated in Figure 4. This SRG is computed over pairs of inputs $u_1(t) = a_1 \sin(\omega t)$, $u_2(t) = a_2 \sin(\omega t)$, where ω is arbitrary and a_1, a_2 are variables in \mathbb{R} .

Truncating the spectrum of the output of a nonlinearity to the fundamental frequency component leads to an underestimation of the action of the nonlinearity, in the following sense.

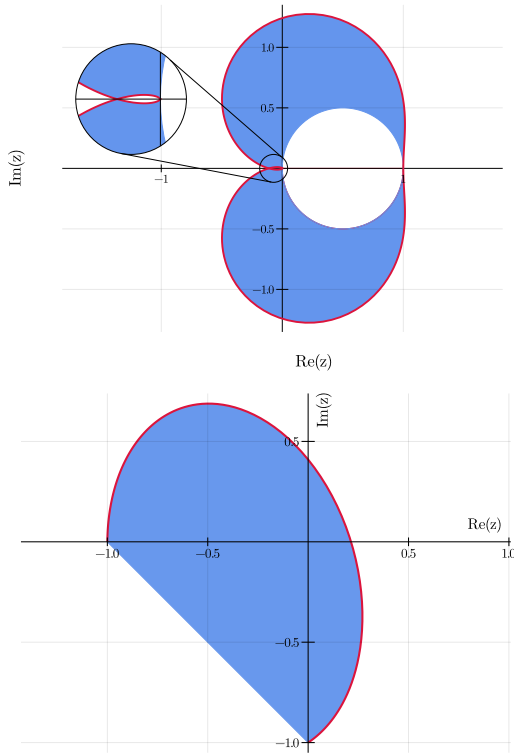


Fig. 3. SRG of the transfer function $1/(s^3 + 5s^2 + 2s + 1)$ (top). The red curve is its Nyquist diagram. The image of the upper half of the SRG under the Beltrami-Klein mapping is shown below.

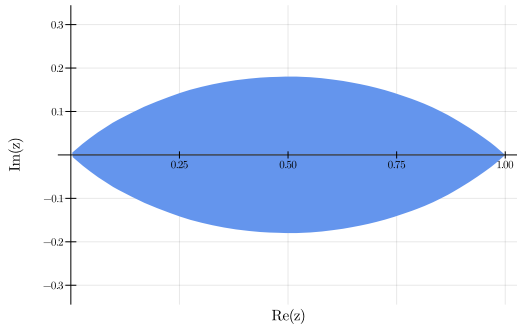


Fig. 4. SRG of the describing function of a saturation over the inputs $u_1(t) = a_1 \sin(\omega t)$, $u_2(t) = a_2 \sin(\omega t)$.

Proposition 4. Given an operator $R: L_2(\mathbb{C}) \rightarrow L_2(\mathbb{C})$ and inputs $u_1(t) = a_1 e^{j\omega t}$, $u_2(t) = a_2 e^{j\omega t}$, we have

$$\begin{aligned} |z_{\text{DF}(R)}(u_1, u_2)| &\leq |z_R(u_1 - u_2)|, \\ \angle((u_1 - u_2), (\text{DF}(R)(u_1) - \text{DF}(R)(u_2))) &\leq \\ &\angle((u_1 - u_2), (Ru_1 - Ru_2)). \end{aligned}$$

Proof. From Bessel's inequality, we have

$$\|Ru_1 - Ru_2\| \geq \|\hat{y}_1(1) - \hat{y}_2(1)\|, \quad (3)$$

where $\hat{y}_1(1), \hat{y}_2(1)$ are the first complex Fourier coefficients of Ru_1, Ru_2 . These are the describing function approximation of R applied to u_1 and u_2 . It follows that the gain of the

describing function approximation is at most the gain of the original function.

Since $u_1 - u_2 = a_0 e^{j\omega t}$, it follows from Parseval's theorem and the orthogonality of $\{e^{jn\omega t}\}_{n \in \mathbb{N}}$ that $\langle u_1 - u_2 | Ru_1 - Ru_2 \rangle = \langle u_1 - u_2 | \text{DF}(R)(u_1) - \text{DF}(R)(u_2) \rangle$. The second inequality then follows from (3) and the fact that acos is monotonically decreasing. \square

A better approximation of the SRG of a nonlinearity can be gained by considering more terms of the Fourier series of the output - this is the technique adopted in higher-order extensions of the describing function [16]. We can also consider a larger class of input signals. Figure 5 shows the SRG of a saturation, computed over the inputs $u_1 = k_1 + a_1 \sin(\omega t)$, $u_2 = k_2 + a_2 \sin(\omega t)$, with the first 10 harmonics of the output calculated.

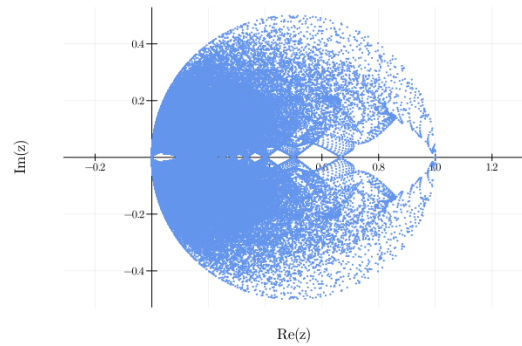


Fig. 5. The SRG of a saturation, computed over a set of inputs of the form $u_1 = k_1 + a_1 \sin(\omega t)$, $u_2 = k_2 + a_2 \sin(\omega t)$, with the output truncated in frequency to the first 10 harmonics.

For differentiable nonlinearities, taking the discretization of the nonlinearity along an input trajectory (that is, the Fréchet derivative of the nonlinearity) gives an approximation of the system behavior at nearby trajectories. Plotting the SRG of the linearization provides another method of approximating the SRG of the original system. For the saturation, taking the linearization along constant trajectories $u(t) \neq -1, 1$ gives either the identity or the zero map - the SRG of the linearization is then the point 0 if $|u(t)| < 1$ or the point 1 otherwise.

B. Bounding the scaled relative graph

The SRG of a system is constrained by its input/output properties. By plotting the SRGs of each system property, we can build a set of geometric constraints on the SRG of the system, using the fact that, for two classes of operators \mathcal{A} and \mathcal{B} , $\text{SRG}(\mathcal{A} \cap \mathcal{B}) \subseteq \text{SRG}(\mathcal{A}) \cap \text{SRG}(\mathcal{B})$. Theorem 4.1 of Ryu, Hannah, and Yin [1] shows that for SRG-full classes, a stronger result holds.

Proposition 5. (Theorem 4.1 [1]): If \mathcal{A} and \mathcal{B} are SRG-full classes, then $\mathcal{A} \cap \mathcal{B}$ is SRG-full, and

$$\text{SRG}(\mathcal{A} \cap \mathcal{B}) = \text{SRG}(\mathcal{A}) \cap \text{SRG}(\mathcal{B}).$$

We demonstrate over-approximation of the SRG again using the example of a saturation. The saturation obeys the

following two slope, or incremental sector, conditions.

$$\begin{aligned} \langle u_1 - u_2 | \text{sat}(u_1) - \text{sat}(u_2) \rangle &\geq 0 \\ \| \text{sat}(u_1) - \text{sat}(u_2) \| &\leq \| u_1 - u_2 \|. \end{aligned}$$

Note that the two conditions above are equivalent to the standard IQC for incrementally sector-bounded nonlinearities. Denoting $u_1(t) - u_2(t)$ by Δu and $y_1(t) - y_2(t)$ by Δy , we have [6, Thm. 2, p.2]:

$$\begin{aligned} &\frac{\Delta y}{\Delta u} \leq 1 \ \& \ \Delta y \Delta u \geq 0 \\ \iff &\Delta y \Delta u \leq \Delta u^2 \ \& \ \Delta y \Delta u \geq 0 \\ \iff &(\Delta y \Delta u - \Delta u^2) \Delta y \Delta u \leq 0 \\ \iff &\Delta y^2 - \Delta u \Delta y \leq 0 \\ \iff &\frac{1}{2} \begin{pmatrix} \Delta u \\ \Delta y \end{pmatrix}^\top \begin{pmatrix} 0 & 1 \\ 1 & -2 \end{pmatrix} \begin{pmatrix} \Delta u \\ \Delta y \end{pmatrix} \geq 0. \end{aligned} \quad (4)$$

Integrating and applying Parseval's theorem, we have the incremental IQC

$$\frac{1}{2} \int_{-\infty}^{\infty} \begin{pmatrix} \Delta \hat{u}(\omega) \\ \Delta \hat{y}(\omega) \end{pmatrix}^\top \begin{pmatrix} 0 & 1 \\ 1 & -2 \end{pmatrix} \begin{pmatrix} \Delta \hat{u}(\omega) \\ \Delta \hat{y}(\omega) \end{pmatrix} d\omega \geq 0,$$

where $\hat{x}(\omega)$ denotes the Fourier transform of $x(t)$.

Equation 4 states that the saturation is 1-cocoercive. It follows from [1, Prop. 3.3] that the SRG of the saturation is contained in the disc with centre $1/2$ and radius $1/2$, as shown in Figure 6.

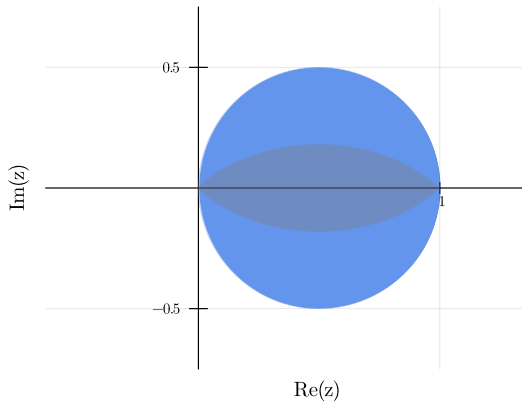


Fig. 6. The SRG of the class of operators which are incrementally positive and have incremental L_2 gain of at most 1. The shadow indicates the SRG of the describing function approximation.

The SRG shown in Figure 6 is SRG-full: if the SRG of a system H lies within this SRG, then H is incrementally passive and has L_2 gain less than or equal to 1.

In the previous section, we showed that sampling the SRG of the saturation appeared to fill the disc with centre $1/2$ and radius $1/2$. Here, we have shown that this region bounds the SRG of the saturation. In the submitted journal version of this paper [15], we have refined this analysis, and shown that the SRG of the saturation is *precisely* the disc with centre $1/2$ and radius $1/2$.

V. SYSTEM ANALYSIS WITH SCALED RELATIVE GRAPHS

Under certain conditions, the SRG of an interconnection of systems is the interconnection of the SRGs of the individual systems. In the same way as the SRG can be used to give intuitive, visual proofs of many standard results in optimization, it can be used to give simple proofs of many classical results in system theory, which rely on the inference of the properties of a system from the properties of its components. We demonstrate this with a simple, graphical proof of the classical incremental passivity theorem.

First, we introduce the necessary interconnection laws (and refer the reader to [1, sec 4] for several other interconnection laws). Given an operator R , we denote by R^{-1} the *relational inverse* of R , that is the map $u \mapsto \{v \mid Rv = u\}$. This map always exists, and coincides with the regular inverse when R is an invertible operator. We define inversion in the complex plane by the Möbius transformation $re^{j\omega} \mapsto (1/r)e^{j\omega}$.

Proposition 6. (Theorem 4.3 [1]): *Given a class of operators \mathcal{A} , $\text{SRG}(\mathcal{A}^{-1}) = (\text{SRG}(\mathcal{A}))^{-1}$.*

A class of operators \mathcal{A} is said to satisfy the chord property if $z \in \text{SRG}(\mathcal{A}) \setminus \{\infty\}$ implies $[z, \bar{z}] \subseteq \text{SRG}(\mathcal{A})$.

Proposition 7. (Theorem 4.4 [1]): *Let \mathcal{A} and \mathcal{B} be SRG-full classes such that either \mathcal{A} or \mathcal{B} satisfies the chord property and $\infty \notin \text{SRG}(\mathcal{A})$ and $\infty \notin \text{SRG}(\mathcal{B})$. Then $\text{SRG}(\mathcal{A} + \mathcal{B}) = \text{SRG}(\mathcal{A}) + \text{SRG}(\mathcal{B})$.*

Propositions 6 and 7 allow a simple, geometric proof of the following incremental form of the classical passivity theorem.

Proposition 8. *The negative feedback interconnection (Figure 7) of two incrementally positive systems H_1 and H_2 , is incrementally positive.*

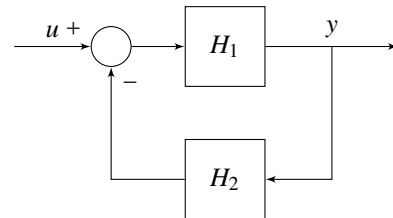


Fig. 7. Negative feedback interconnection of H_1 and H_2 .

Proof. The negative feedback interconnection of H_1 and H_2 may be written as

$$y \in (H_1^{-1} + H_2)^{-1}(u).$$

The proof by SRG shows that the sequence of operations that take H_1 to this form leave the right half plane $\mathbb{C}_{\text{Re} \geq 0}$ invariant. In particular, note that $\text{SRG}(\mathcal{M}) = \mathbb{C}_{\text{Re} \geq 0}$, and $\text{SRG}(H_1) \subseteq \text{SRG}(\mathcal{M})$. Furthermore, \mathcal{M} is SRG-full and obeys the chord condition. Now,

- 1) $\text{SRG}(\mathcal{M}^{-1}) = (\mathbb{C}_{\text{Re} \geq 0})^{-1} = \mathbb{C}_{\text{Re} \geq 0}$;
- 2) $\text{SRG}(\mathcal{M}^{-1} + \mathcal{M}) = \mathbb{C}_{\text{Re} \geq 0} + \mathbb{C}_{\text{Re} \geq 0} = \mathbb{C}_{\text{Re} \geq 0}$;
- 3) $\text{SRG}(\mathcal{M}^{-1} + \mathcal{M})^{-1} = (\mathbb{C}_{\text{Re} \geq 0})^{-1} = \mathbb{C}_{\text{Re} \geq 0}$. \square

VI. CONCLUSIONS

This paper has presented preliminary results applying the scaled relative graph of Ryu, Hannah, and Yin [1] to system analysis. The SRG is a generalization of the classical Nyquist criterion which may be plotted for any operator on L_2 , not only those that are linear and time invariant. This opens many opportunities to revisit classical analysis and control design techniques in terms of the SRG, and extend linear techniques to nonlinear operators. We have made a preliminary step in this direction by presenting a simple, graphical proof of the passivity theorem.

A particularly promising avenue is the extension of LTI stability and robustness techniques to nonlinear operators via the SRG, beginning with a generalization of the Nyquist criterion for stable operators. The SRG allows the gain and phase margins to be calculated for nonlinear operators. This approach to nonlinear system analysis is explored in the submitted journal version of this paper [15].

REFERENCES

- [1] E. K. Ryu, R. Hannah, and W. Yin, "Scaled relative graphs: Nonexpansive operators via 2D Euclidean geometry," *Mathematical Programming*, 2021. DOI: 10.1007/s10107-021-01639-w.
- [2] X. Huang, E. K. Ryu, and W. Yin. (2020). "Tight Coefficients of Averaged Operators via Scaled Relative Graph." arXiv: 1912.01593 [math].
- [3] H. Nyquist, "Regeneration theory," *The Bell System Technical Journal*, vol. 11, no. 1, pp. 126–147, 1932. DOI: 10.1002/j.1538-7305.1932.tb02344.x.
- [4] A. El-Sakkary, "The gap metric: Robustness of stabilization of feedback systems," *IEEE Transactions on Automatic Control*, vol. 30, no. 3, pp. 240–247, 1985. DOI: 10.1109/TAC.1985.1103926.
- [5] G. Vinnicombe, *Uncertainty and Feedback: H_∞ Loop-Shaping and the v -Gap Metric*. Imperial College Press, 2000, ISBN: 978-1-86094-163-4.
- [6] C. A. Desoer and M. Vidyasagar, *Feedback Systems: Input–Output Properties*. Elsevier, 1975. DOI: 10.1016/B978-0-12-212050-3.X5001-4.
- [7] N. S. Krylov and N. N. Bogoliubov, *Introduction to Non-Linear Mechanics*. Princeton: Princeton University Press, 1947, ISBN: 978-0-691-07985-1.
- [8] A. Blagquière, *Nonlinear System Analysis*. Academic Press, 1966.
- [9] J.-J. E. Slotine and W. Li, *Applied Nonlinear Control*. Englewood Cliffs, N.J: Prentice Hall, 1991, 459 pp., ISBN: 978-0-13-040890-7.
- [10] A. Pavlov, N. van de Wouw, and H. Nijmeijer, "Frequency response functions and Bode plots for nonlinear convergent systems," in *Proceedings of the 45th IEEE Conference on Decision and Control*, San Diego, CA, USA: IEEE, 2006, pp. 3765–3770. DOI: 10.1109/CDC.2006.377669.
- [11] C. Chen, D. Zhao, W. Chen, S. Z. Khong, and L. Qiu. (2020). "Phase of Nonlinear Systems." arXiv: 2012.00692 [cs, eess, math].
- [12] A. van der Schaft, *L_2 -Gain and Passivity Techniques in Nonlinear Control*, ser. Communications and Control Engineering. Cham: Springer International Publishing, 2017, ISBN: 978-3-319-49991-8.
- [13] A. Megretski and A. Rantzer, "System analysis via integral quadratic constraints," *IEEE Transactions on Automatic Control*, vol. 42, no. 6, pp. 819–830, 1997. DOI: 10.1109/9.587335.
- [14] X. Huang, E. K. Ryu, and W. Yin. (2020). "Scaled Relative Graph of Normal Matrices." arXiv: 2001.02061 [cs, math].
- [15] T. Chaffey, F. Forni, and R. Sepulchre. (2021). "Graphical Nonlinear System Analysis." arXiv: 2107.11272 [cs, eess, math].
- [16] P. W. J. M. Nuij, O. H. Bosgra, and M. Steinbuch, "Higher-order sinusoidal input describing functions for the analysis of non-linear systems with harmonic responses," *Mechanical Systems and Signal Processing*, vol. 20, no. 8, pp. 1883–1904, 2006. DOI: 10.1016/j.ymsp.2005.04.006.